KCI Concrete Journal
Vol. 13 No. 2 pp. 33-41, July 2001

Assessment of Fracture Behaviors for CIP Anchors Fastened to Cracked and Uncracked Concretes

Young-Soo Yoon,[1] Ho-Seop Kim,[1] and Sang-Yun Kim[2]

[1] Department of Civil & Environmental Engineering, Korea University, Korea
[2] Structural Systems & Site Evaluation Department, Korea Institute of Nuclear Safety, Korea

(Received June 5, 2001, Accepted July 30, 2001)

Abstract

This paper presents the crack effect on CIP anchors and prediction of tensile capacity, as governed by concrete cone failure. Single anchors where located at center of concrete specimen. Three different types of cracks such as crack width of 0.2 ㎜ and 0.5 ㎜, crack depth of 10 ㎝ and 20 ㎝, and crack location of center and off-center point were simulated. Static tensile load was applied to 7/8-in. CIP anchors of 10 ㎝ and 20 ㎝ embedment length in concrete with compressive strength of 280 kgf/㎠. Tested pullout capacities were compared to the values determined using current design methods (such as ACI 349-97, ACI 349 revision and CEB-FIP which is based on CCD Method). The comparison of CCD Method and ACI revision showed almost the same values in uncracked concrete specimen. In cracked concrete, CCD Method predicted conservative values. Three-dimensional non-linear FEM modeling also has been performed to determine the stresses distribution and crack inclination.

Keywords: CIP anchors, cracked concrete, failure mode, ACI 349, CCD method

1. Introduction

Cast-in-place anchors are in general used to connect structural members and equipment, safely and economically, to concrete or masonry. Especially in the nuclear power plant, the safe fastening is indispensable because of the design service life over 30 years and complicated construction. For economic and safe installations, the concrete anchor system should be designed to maintain the seismic load as well as the static and dynamic loads through the whole service life. It is, also, indispensable to consider the crack effect since these structures are made of concrete. The external loads, internal thermal expansion, and shrinkage and creep help crakes develop. Therefore, it may be safely assumed that concrete structures always have developed cracks. The design excluding concrete crack effect yields the lower safety factor and assesses a higher strength than the real strength that may result in an unsafe design. Hence the designer must consider the influence of concrete cracks into the design of concrete anchor system.

In cracked concrete, the stress distribution changes as shown in Fig. 1. These changes in distribution result in reduced strength and different failure mode compared to that of uncracked concrete.[1]

The behavior of an anchor under tensile load can be altered because not only of concrete cracks but also of type of anchors. As shown in Fig. 2 the existing crack under tensile load gives larger displacement and decreased tensile capacity of an anchor.[2] To consider these concrete crack effects the crack coefficients are used in codes.

Based on experimental data, the CCD Method (Concrete Capacity Design Method) was presented based on concrete fracture mechanics approach.[3] This design method provides very close comparison with experimental data by using a 35-degree breakout cone and the size effect. The ACI 349 committee shows new revision.[4, 5]

The objective of this research was to present the experimental data and recommend design method needed for safe and economical design of a single CIP anchor system in cracked and uncracked concrete.

By simulating various types of concrete cracks that can be easily developed in any concrete the investigation of crack effects on the CIP anchor was carried out. By comparison test results to values predicted by existing design codes and by the finite element analysis, the appropriateness of the design codes in cracked concrete was estimated.

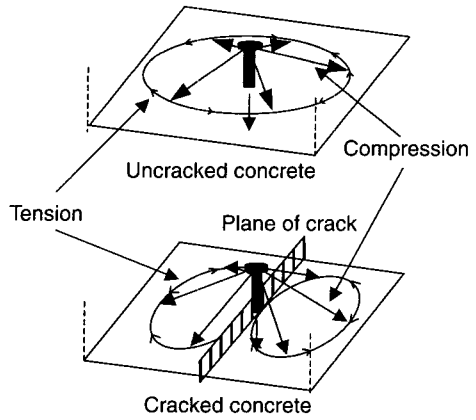

Fig. 1 Stress distributions in cracked and uncracked concretes

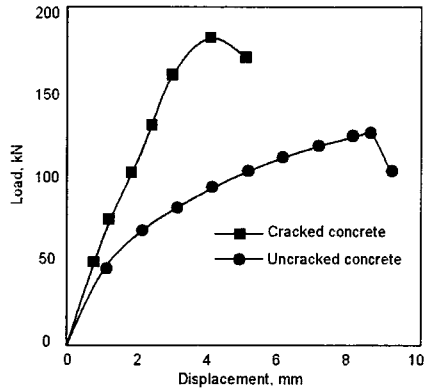

Fig. 2 Load-displacement curves of CIP anchor under static tensile load installed in cracked and uncracked concrete

2. Background Theory

2.1 CIP Anchors

Cast-in-place anchors are placed in position before concrete is cast. A cast-in-place anchor can be a headed bolt of standard structural steel, placed with its head in the concrete. It can also be a standard threaded rod and a hexagonal nut, with the nut embedded in concrete. Finally, it can be a bar bent at one end and threaded at the other end, with the bent end placed in concrete. Fig. 3 shows these variations. A headed cast-in-place anchor depends on mechanical interlock and bearing on concrete of the bolted head for load transfer. Some bond may also exist between the anchor shank and surrounding concrete.

2.2 Definition of Embedment Depth

The effective embedment depth of a CIP anchor is the distance between the concrete surface and the bearing portion of the anchor head.

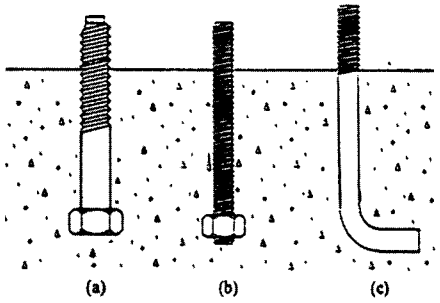

Fig. 3 Typical cast-in-place anchors

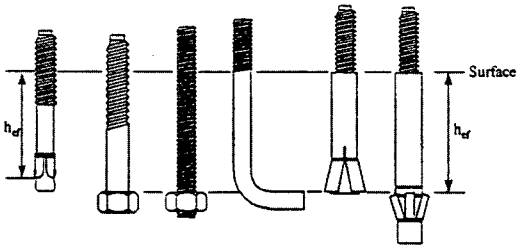

Fig. 4 Definitions of embedment depths

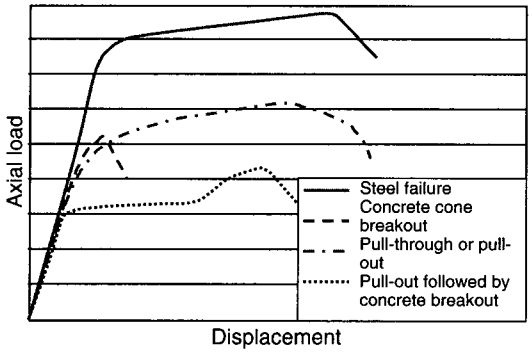

Fig. 5 Typical load-displacement curves of different failure modes in tension[2]

2.3 Behavior of Single Anchor Connected to Concrete

Depending on the diameters of a CIP anchor, embedment depths and compressive strength of concrete, different load-displacement behavior can be determined for a tensile test as shown in Fig. 5.[2]

There are several types of tensile failure modes, which are steel failure, concrete cone breakout, pullout failure, pull-through failure, splitting failure and lateral blowout failure under tensile load.

Concrete breakout failure occurs by the propagation of a roughly conical fracture surface from the bearing edge of the anchor head of a cast-in-place anchor, or from the tip of the expansion mechanism of an expansion or an undercut anchor. The angle of the cone, as measured from the concrete surface, increases from around 35 degree at shallow embedments, to about 45 degree at deep embedments.

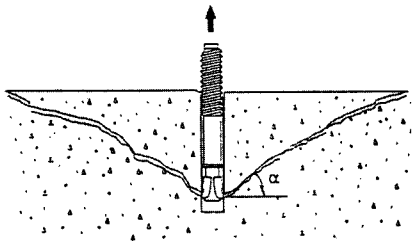

Fig. 6 Concrete breakout failure

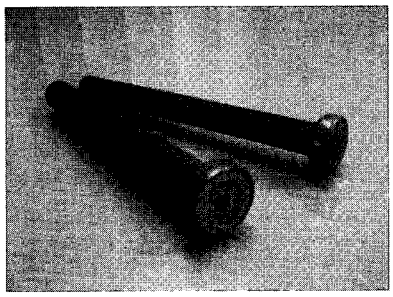

Fig. 7 CIP anchor used for tests

2.4 Effect of Cracks on Anchor Capacity

In general, cracks lower the tensile capacity of a CIP anchor because the crack interrupts the stress field in concrete surrounding the anchor, thereby altering the stresses distribution in concrete. Although the scatter of the test results is rather large, the reduction of ultimate load of concrete breakout generally increases with initial crack width. A numerical modeling showed that the concrete breakout capacity decreases with increasing crack width up to 0.15mm, to approximately 70% of the full breakout capacity for cast-in-place anchors.[1]

3. Test Program

3.1 Introduction

To evaluate the effect of cracks on CIP anchors, where various types of concrete cracks were simulated and static tensile load was applied. The load-displacement curves, failure modes and failure strengths were investigated.

3.2 Test Variables

In tensile testing of a CIP anchor there are many test variables to consider such as loading types, embedment depth, edge distances, anchor types, single or multiple number of anchors, distances between anchors, cracked and uncracked concrete, concrete strengths and existing reinforcement. Because the main objective was to evaluate the crack effects on the anchor pullout behavior test was focused on the cracks. The specimen size was 70cm×70cm×20cm and a total of 20 specimens including spare specimens were prepared. The same test was repeated at least three times per each test variable as shown in Table 1.[1, 6-8]

Table 1 Test groups and test variables

Test group	Crack width	Crack depth	Crack location
No crack	-	-	-
0.5mm crack	0.5 ㎜	20 ㎝	Center
0.2mm crack	0.2 ㎜	20 ㎝	Center
Side crack	0.5 ㎜	20 ㎝	Off-center
Half crack	0.5 ㎜	10 ㎝	Center

Table 2 Concrete strength

Strength (kgf/cm^2)	7 day compressive strength	28 day compressive strength	28 day splitting tensile strength
Average of tests	193	286	21

3.3 Material Properties

The CIP anchor, which is used in Korean nuclear power plant, is similar to that used in the NRC (U. S. Nuclear Regulatory Commission). Usually anchors with diameters ranging between 9.2mm~25.4mm are used in the nuclear power plant. A 7/8-inch (2.22mm) Headed CIP anchor was used for test because anchors with diameters larger than 1 inch are not frequently used in Korea.

Usually in nuclear power plants in Korea the concrete strength ranges between 280 kgf/cm^2 and 400 kgf/cm^2, although sometimes concrete of 210 kgf/cm^2 strength can be used. The nominal strength of a ready mixed concrete used in this test was 280 kgf/cm^2. Table 2 shows the concrete cylinder test results.

In order to control cracks, reinforcing bar of 10 ㎜ diameter and yield strength of 3000 kgf/cm^2 were used. Eight bars were used for each direction, and a total of 16 bars was placed with reinforcement ratio of 0.45. Details for the reinforcement and the anchor placement are presented in Fig. 8 and 9.

3.4 Test Equipment

The loading capacity of the UTM was 200 tonf with the dimensions as shown in Figure 10. Because of the size limitation of the UTM, one anchor was embedded in one concrete specimen. To connect the test specimen to the UTM a special concrete yoke was fabricated.

The inner size of the concrete yoke was 70cm ×70cm ×50cm and made of thick steel plate over 2.5cm thick in order to resist large loads. The bolts and nuts for connecting plates were made of strong enough to resist yield strength

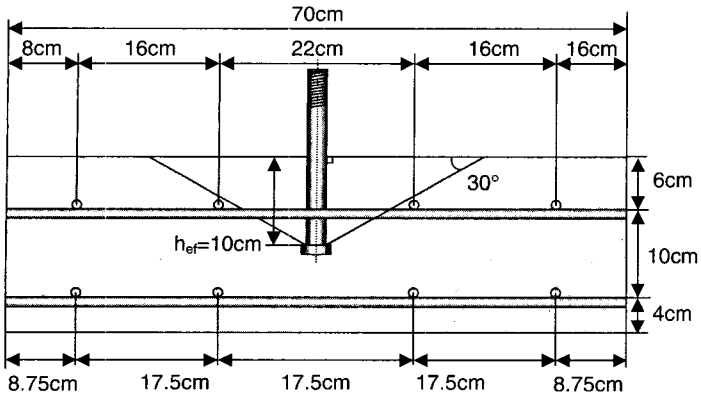

Fig. 8 Reinforcements and anchor placement (cross-sectional view)

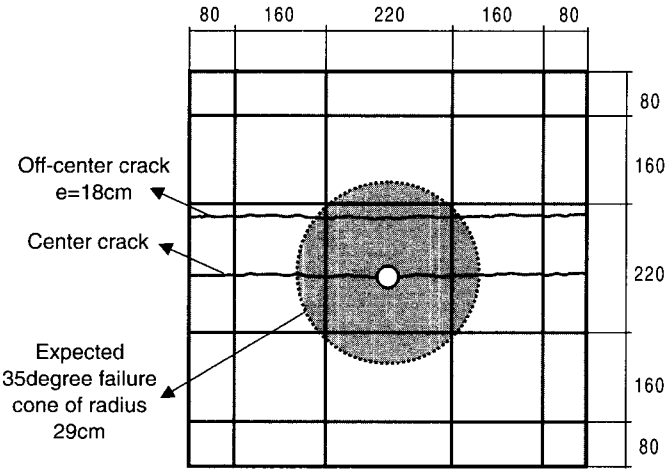

Fig. 9 Reinforcements and anchor placement (plan view)

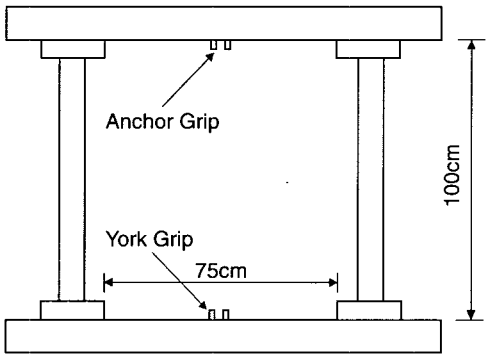

Fig. 10 UTM

of an anchor. The top cover of yoke is opened and 6 cm closed plates from each edge actually will be supports.

Cracks in concrete were created using a wedge splitter. The splitter, especially designed to simulate artificial cracks had 28cm length and 20mm inner diameter. It consists of three parts; splitting tube of two parts and wedge splitter as shown in Fig. 12. The splitting tube can be separated into two parts and installed in a direction that can be changed along crack direction as desired.

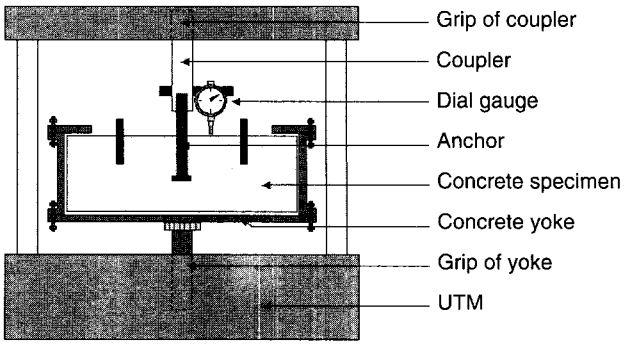

Fig. 11 Test machine

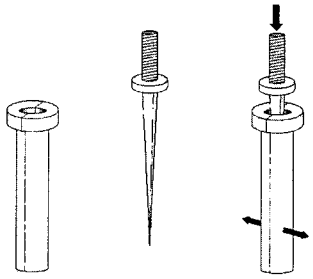

Fig. 12 Crack inducers

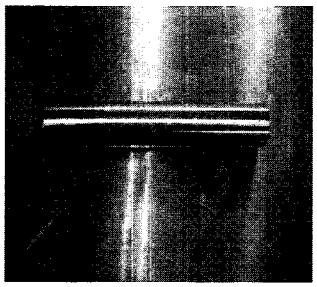

Fig. 13 Coupler

3.5 Test Procedure

Yoke was fastened to the UTM using a thick steel bar attached the bottom of a yoke and the grip equipment of UTM: the steel bar was fastened to the grip part of UTM. Before placing concrete, 3.5 cm thick wooden plate was used to fix the position of a CIP anchor in concrete. After drilling a whole in the wooden plate an anchor was installed through the hole with nuts. The nuts controlled the embedment depths.

Because of the limited length of an anchor(20cm) some extension device was needed in order to fasten the anchor to the UTM grip. For this extension a special coupler was used. This coupler had 10cm inner diameter and was 70cm long as shown in Fig. 13.

In order to install the crack-developing devices, drilling and hammering after inserting the splitting tube and the wedge splitter were needed. Once the crack was created, the crack width was measured. If developed crack width was

determined too wide, the width was decreased by pulling the splitter back with a hydraulic jack.

Reinforcing bars were placed in order to control the crack width. Reinforcements were placed outside the estimated failure zone.

Tensile load was applied to the anchor, and tensile capacity, load-displacement response were measured.

4. Failure Capacity Prediction

There are no codes about concrete anchor in Korea. Therefore test results were compared using existing codes such as ACI349-97, ACI349-97 Revision and CEB-FIP that is based on CCD Method.

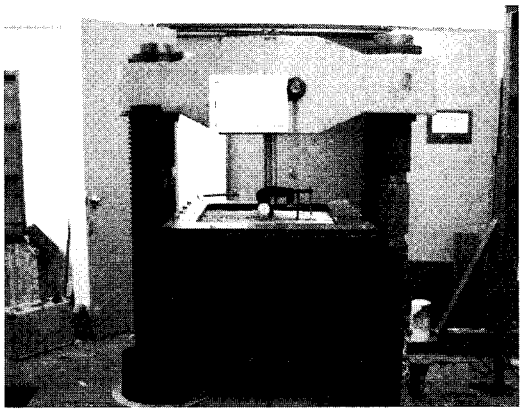

Fig. 14 Test machine setup

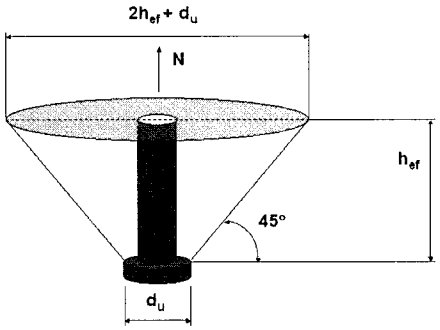

Fig. 15 Concrete tensile breakout cone in ACI 349-97

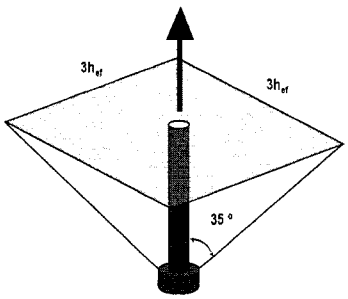

Fig. 16 Tensile concrete breakout cone in CCD method

4.1 ACI349-97

Under tensile load, ACI349-97 limits the yield strength of anchors to be less than the concrete tensile strength in order to induce the ductile failure. When the strength of concrete is less than tensile capacity of anchors it is recommended to place reinforcements.

45-degree cone assumes that a constant tensile stress of $4(f_c)^{1/2}$ acts on the projected area of a cone radiating towards the free surface from the bearing edge of the anchor. Figure 15 shows concrete tensile breakout cone idealized in ACI 349-97.[4]

4.2 ACI349-97 Revision

The revised ACI349-97 follows the failure cone model and concept of CCD Method. Under tensile loading, the concrete capacity of a single fastener is calculated assuming an inclination angle between the failure surface and the surface of the concrete member of about 35 degree.[5] .

4.3 CCD Method

CCD Method considers tensile stress of concrete, breakout area and concrete size effect. This assumes that under tensile loading, the concrete capacity of a single fastening is calculated assuming an inclination between the failure surface and the surface of the concrete member of about 35 degree. The Fig. 16 presents the pyramid-shape concrete breakout idealized in CCD Method.

5. Test Result

The results of monotonic tension test are shown in Table 4. The anchor displacements in each test group are not iden-

Table 3 Prediction of tensile capacity by codes

Code	Uncracked concrete	Cracked concrete
ACI 349	6.51 tonf	4.98 tonf
CCD method	6.73 tonf	4.81 tonf
ACI revision	6.73 tonf	5.38 tonf

Table 4 Test result

Test group	N_{test}
No cracks	7595 kgf
0.5mm crack	5918 kgf
0.2mm crack	6358 kgf
Half crack	6367 kgf
Side crack	6520 kgf

tical because the concrete breaking did not occur at a time but gradually occurred as the crack progressed.

In comparison, 0.2mm crack has 6.9% greater capacity than 0.5mm crack (0.2mm Crack vs 0.5mm Crack). Off-center crack has 9.2% greater capacity than when the case crack is located at center of specimen (0.5mm Crack vs Side Crack). When comparing the crack depths of 20cm and 10cm, 10cm depth crack group has 7.1% greater capacity than 20cm. Therefore wider and deeper crack that is located near the anchor adversely affects the tensile capacity.

Although, the many different failure modes of an anchor can be classified into three cases such as concrete cone breakout failure, concrete pryout failure, steel failure, pull-through failure, and pullout failure, there were only concrete cone breakout failures in this test. The size of failure cone was bigger than that theoretically estimated cone size. The cone size is related to the failure angle. The radius of the cone using the 45° of ACI code was 22cm and one by 35° of CCD Method was about 30cm. The average radius from all tests was 53cm that was larger than these values.

Fig. 23 shows a typical failure shape determined in this test. As shown in Fig. 23 at the head part of anchor, the angle has a range of 45~55° that is similar to the code recommendations. But cracks located at the adjacent of the specimen surface, the failure angle becomes small and it makes larger failure cone. Therefore when designing the anchor system, these large cone, and small angel must be considered in.

6. FEM Analysis

Three dimensional finite element analyses were performed to simulate the fracture behavior of the CIP anchor.[9] The finite element analysis program, ABAQUS / Standard and ABAQUS/CAE was used. In order to consider the material non-linearities of concrete and the anchor, *CONCRETE and *PLASTIC models in ABAQUS/ Standard were used.[10] As a result of analyses, stress contours, crack directions, and tensile capacities were obtained. To find out the crack effect, a "cracked" concrete model was produced, analyzed and compared to the "uncracked" concrete model. Strength reduction and stress distribution due to cracks were also compared and analyzed.

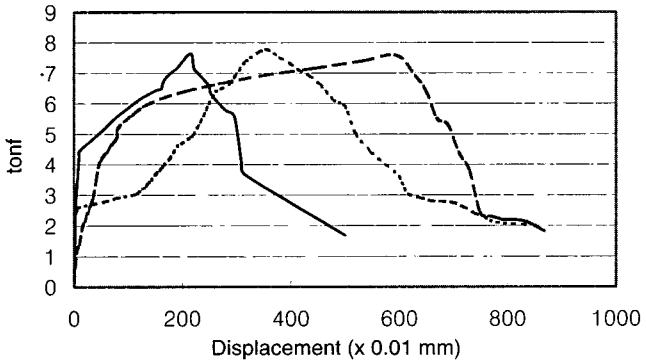

Fig. 17 Load-displacement plots, no cracks

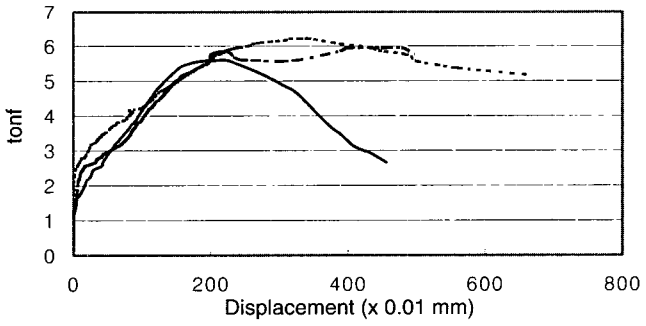

Fig. 18 Load-displacement plots, 0.5mm crack

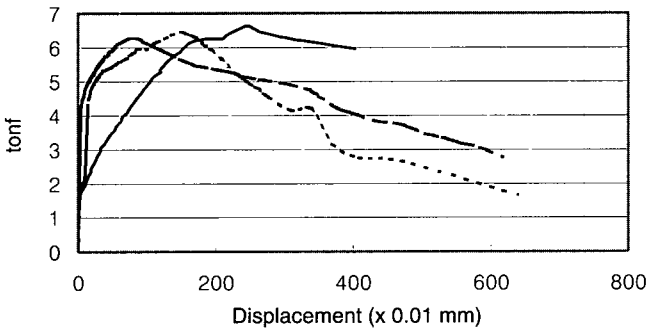

Fig. 19 Load-displacement plots, 0.2mm crack

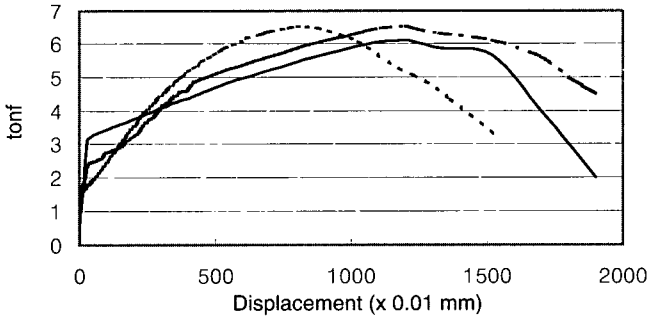

Fig. 20 Load-displacement plots, half crack

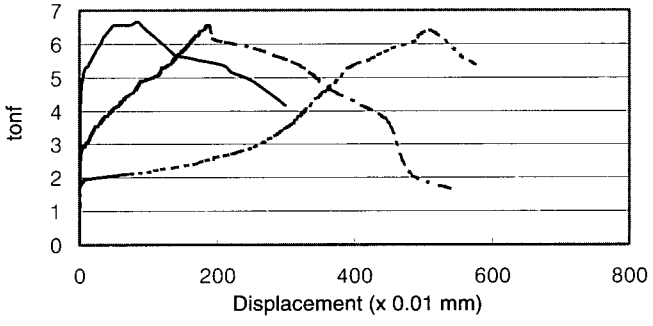

Fig. 21 Load-displacement plots, side crack

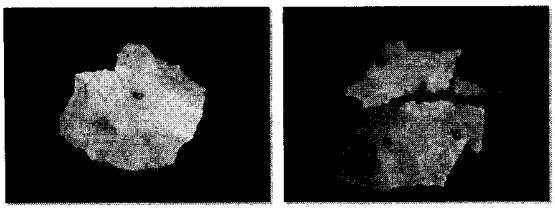

(a) No cracks (b) 0.2mm crack

(c) 0.5mm crack (d) Side crack

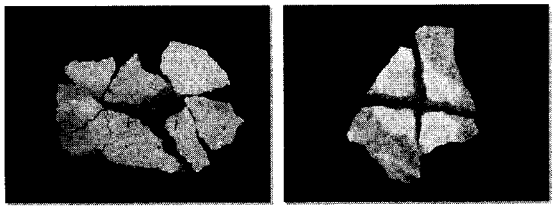

(e) Side crack (f) Half crack

Fig. 22 Failure modes in each test group

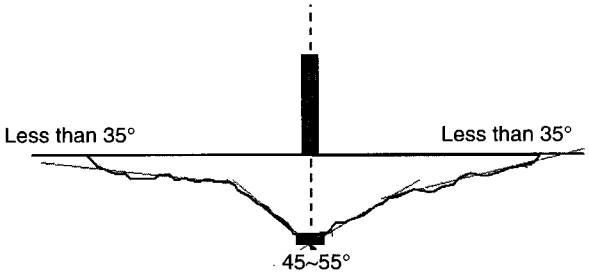

Fig. 23 Resultant failure shape (side view) and failure angle

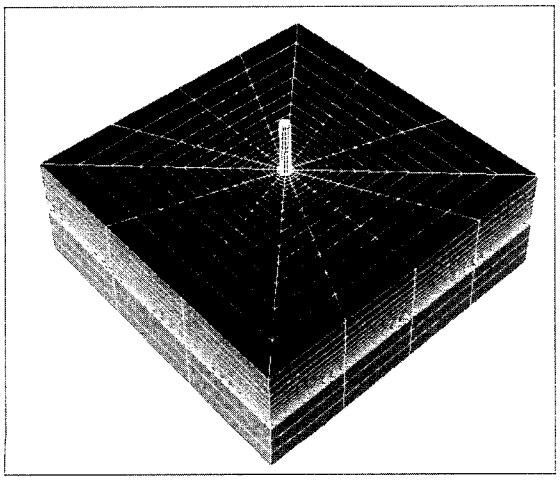

Fig. 24 Three dimensional mesh used in model

A denser mesh was used near the vicinity of the anchor head because of the stress concentration and this is presented in Fig. 24. The principal compressive stress distribution is shown in Fig. 25. Stresses were concentrated near the anchor head and relatively large stresses developed in anchor body compared to concrete. Because the fracture behavior was governed by concrete, anchor did not fail. Fig. 26 and 27 show principal compressive and tensile stress distribution in concrete, respectively. The concrete cracks developed in the normal direction to this principal tensile stress direction. Therefore the direction of principal compressive stress was the same as the direction of crack initiation. The magnitude and direction of the principal compressive stress is represented as the length and inclination of lines in Fig. 26 and 27.

Fig. 28 shows stress (S33) distribution and stress concentration generated near the head. After the crack development, the friction was ignored at interface between the concrete and the anchor surface. In Fig. 31, the stress contour of concrete near the anchor is presented and relatively low stresses spread broadly over the concrete.

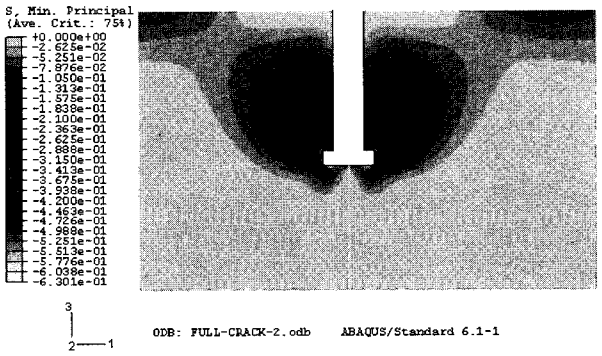

Fig. 25 Principal compressive stress contour in concrete

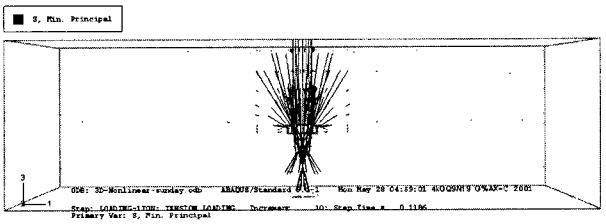

Fig. 26 Direction of principal compressive stress in concrete

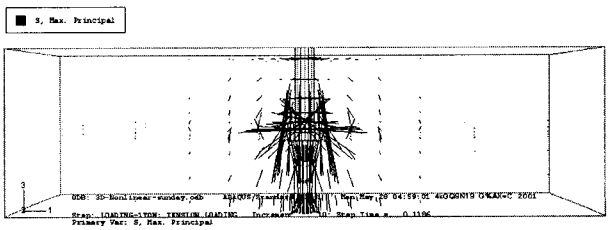

Fig. 27 Direction of principal tensile stress in concrete

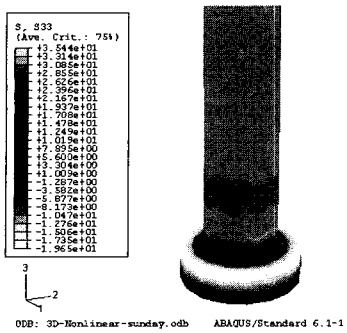

Fig. 28 Stress (S33) contour of anchor

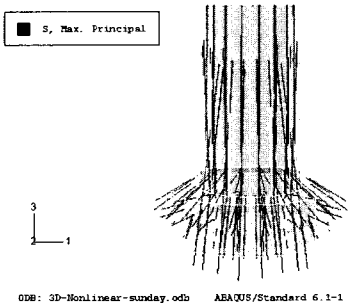

Fig. 29 Principal tensile stress distribution of anchor

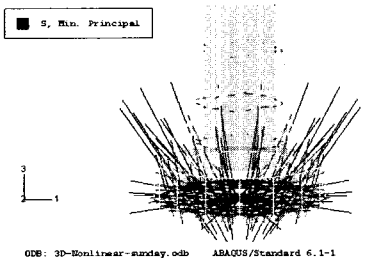

Fig. 30 Principal compressive stress distribution of anchor

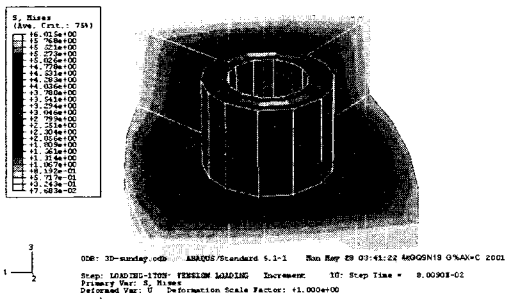

Fig. 31 Stress (S33) contour in concrete near anchor head

Fig. 29 and Fig. 30 show the principal tensile and compressive stress distributions. The line length and the line inclination represent the magnitude of principal stresses and the direction of principal stresses, respectively.

Eventually, the anchor bolt is almost entirely subjected tensile load but the stresses distributed are separated into the compression zone and the tensile zone. Severe compressive stress is distributed over the top face of the head and the tensile stress is broadly distributed over the anchor.

Table 5 Test result and comparison with code predictions

Test group (unit: kgf)	No cracks	0.5mm crack	0.2mm crack	Half crack	Side crack
N_{test}	7595	5918	6358	6367	6520
N_{ACI349}	6508	4977	4977	4977	4977
$N_{ACI\,R}$	6728	5384	5384	5384	5384
$N_{CCD\ Method}$	6731	4808	4808	4808	4808
N_{FEM}	6947	5002	5002	5002	5002
N_{test}/N_{ACI349}	1.167	1.189	1.277	1.279	1.310
$N_{test}/N_{ACI\,R}$	1.129	1.099	1.181	1.183	1.211
$N_{test}/N_{CCD\ Method}$	1.128	1.231	1.322	1.324	1.356
N_{test}/N_{FEM}	1.093	1.183	1.271	1.273	1.303

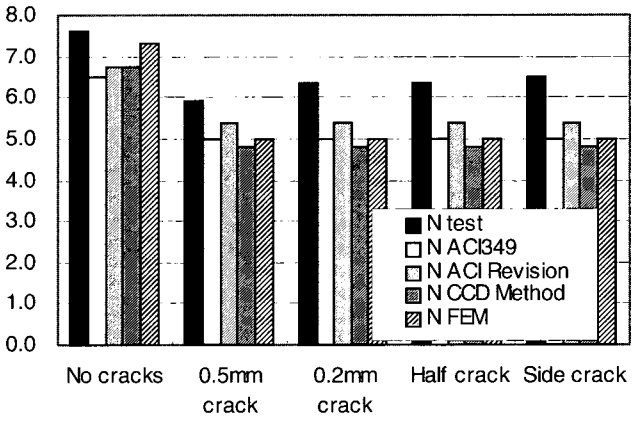

Fig. 32 Tensile capacity comparisons

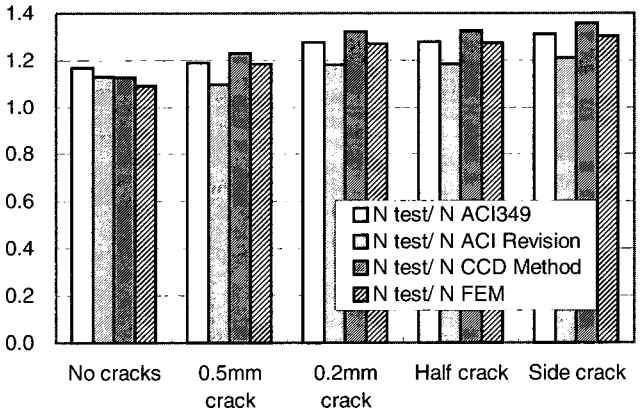

Fig. 33 $N_{test}/N_{predict}$ comparisons

As can be seen in the principal stress direction, the crack initiation angle is about 35 to 45 degrees. Therefore the presented angles of a cone breakout suggested in codes are appropriate. However, the principal compressive stress contour in Fig. 25 suggests that the breakout model does not exactly coincide with the perfect cone.

7. Comparison of Results

The test result predicted values using codes and FEM

analysis results are presented in Table 5 and Fig. 32 and 33. FEM Crack Modeling was performed only for the case of central cracks of 1mm width and of 20cm depth. ACI 349 and CCD Method consider the crack effect importing one crack coefficient. Therefore analysis of tensile capacity in cracked concrete was performed with an assumption of inferior crack condition in order to make better comparisons with codes. The prediction by revised ACI 349 shows close agreement with the test result. In the case of uncracked concrete, there are almost no differences between the value predicted by the CCD Method and the revised ACI 349-97 because of the similar design concept. For cracked concrete, codes show conservative values. Therefore based on this study of results, for the design of the CIP anchor in cracked and uncracked concrete, the revised ACI 349-97 method is recommended.

8. Conclusions

The following conclusions were drawn from the results of the limited number of experimental data and the analytical study of the CIP single anchors :

1. Most critical crack was the one that passes through the installed anchor. As the crack progressed deeper and wider the anchor showed sudden drops in the tensile capacity.
2. ACI 349-97 and CCD Method showed a safety margin for the tensile capacity prediction of the CIP anchors (of 22mm diameter, 20cm length and 10cm embedment length) in cracked and uncracked concrete sections.
3. In cracked section, the CCD Method showed excessive conservativeness for the tensile capacity. The revised ACI 349-97 is most appropriate.
4. Three-dimensional modeling of an anchor installed in uncracked concrete predicted relatively accurate tensile capacity. In the case of cracked concrete, tensile capacities predicted by F.E.M analyses were similar to those determined using code equations.

References

1. Eligehausen, R. and Balogh, T., "Behavior of Fasteners Loaded in Tension in Cracked Reinforced Concrete," ACI Structural Journal, Vol. 92, No. 3, May-June, 1995, pp. 365-379.
2. Cook, R. A., Collins, D. M., Klingner, R. E., and Polyzois, D., "Load-Deflection Behavior of Cast-in-Place and Retrofit Concrete Anchors," ACI Structural Journal November-December, 1992, pp.639-649.
3. Fuchs, W., Eligehausen, R., and Breen, John E., "Concrete Capacity Design (CCD) Approach for Fastening to Concrete," ACI Structural Journal, Vol.92, No. 1, Jan.-Feb. 1995, pp. 73-94.
4. ACI 349 Appendix B Draft, Fastening to Concrete *06/16/99*
5. ACI 349 Proposed Revisions to "Code Requirements for Nuclear Safety Related Concrete Structures and Commentary," New Appendix B, Fastening to Concrete
6. ASTM, "Standard Specification for Performance of Anchors in Cracked and Non-cracked Concrete Element," Draft 1, Mar. 22, 1993.
7. ASTM E06.13-Z5819Z Draft 4, Standard Specification for Performance of Anchors in Cracked and Uncracked Concrete Elements.
8. ASTM E488-96, Standard Test Method for Strength of Anchor in Concrete and Masonry Elements, pp. 57-64.
9. Dalati, R. El, Berthaud, Y., Mesureur, B., and Ghassan M., "Three-Dimensional Modeling of Anchorage Subject to Shear Loads," ACI Structural Journal, May-June, 2000, pp. 408-417.
10. Hibbitt, Karlsson & Sorensen INC, ABAQUS/Standard User's Manual, ABAQUS/Theory Manual.